2007 IEEE International Conference on
Robotics and Automation
Roma, Italy, 10-14 April 2007

Pinpointed control of muscles by using power-assisting device

Jun Ueda, Ming Ding, Masayuki Matsugashita, Reishi Oya, Tsukasa Ogasawara

Abstract— **The aim of this paper is to arbitrarily modify the load force of any selected muscle by using an exoskeleton, thus enabling "pinpointed" motion support, rehabilitation, and training. An advanced dynamic model, called a musculoskeletal-exoskeletal integrated human model, is developed. The driving-forces of the pneumatic actuators are designated by a muscle force control algorithm using the integrated model. A prototype power-assisting system is developed using pneumatic rubber actuators. The feasibility of the muscle force control is analyzed from a view point of nonlinear programming. The validity of the method is confirmed by measuring surface electromyographic signals of related muscles.**

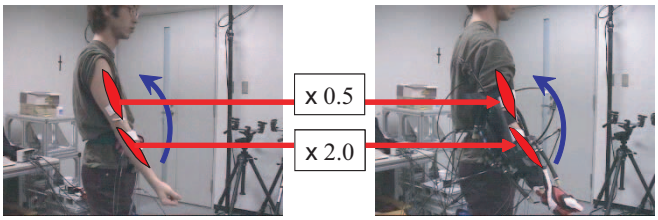

Fig. 1. Concept of Muscle Force Control

I. Introduction

For the upcoming aging society, a power-assisting system is considered an important robotic technology for enhancing the mobility of elderly and disabled people. Other potential applications are for rehabilitation and sports training. A wide variety of power-assisting devices have been studied in terms of mechanism and control[1][2]. The main focus of these devices is to assist human motion as a whole, reducing the burden of all related muscles, such as for walking or lifting a patient. However, if we consider muscle rehabilitation or motion support for people whose specific muscles are weak, it is considered effective to support the specific muscles selectively, in order not to impair the functionality of other healty muscles. This implies that a more detailed power-assisting is required, i.e., power-assisting at the individual muscle level, enabling "pinpointed" muscle control for effective muscle rehabilitation and training.

It is well-known that a human body has a larger number of muscles than that of joints. This fact makes the estimation of muscle forces difficult since the solution of muscle forces is nonunique for a certain motion. This problem can be solved by minimizing an empirical cost function proposed by Crowninshield *et al*[3]. Our concept is to obtain a desired combination of muscle forces by activating a power-assist device in consideration of Crowninshield's cost minimization. To the author's knowledge, there has been no study on the control of power-assisting devices in terms of this perspective. Figure 1 briefly shows the concept for elbow exercise, in which the load foces of two selected muscles are modified in different ratios by wearing a power-assisting device.

We propose a muscle force control algorithm that checks the feasibility of a desired combination of muscle forces, and calculates the driving-force of the power-assisting device for realizing the desired muscle forces. The feasibility of this muscle force control is analyzed from a view point of nonlinear programming. This analysis provides a feasible set of muscle forces obtained by the power-assisting. An advanced dynamic model, called a musculoskeletal-exoskeletal integrated human model, is developed for this calculation. Furthermore, a prototype power-assisting system has been developed for assisting the upper-right limb of a subject. Pneumatic rubber actuators are applied to this power-assisting system for compactness as well as for safety reasons. The validity of the method has been confirmed by simulations and experiments. Surface electromyographic (EMG) signals of related muscles with and without power-assisting device are measured. Experimental results indicate that our approach is promising.

II. Musculoskeletal-exoskeletal integrated human model

A. Musculoskeletal model

A musculoskeletal dynamic model of the human upper right limb has been developed as shown in Fig. 2. This model consists of 5 rigid links with 13 joints corresponding to the waist, neck, shoulder, elbow, and wrist. 51 muscles of the upper-right limb are modeled by massless wires [4] [5]. Points of muscle attachment (origins and insertions) are determined from anatomical data [4]. This model does not include a detailed model of the hand; the insertions of the muscles for finger flexion/extension are set to extensor retinaculum and flexor retinaculum to simplify the model.

The validity of the musculoskeletal model is evaluated by comparing the muscle moment arms given by our model and the approximate expressions given by Lemay *et al.* [6].

Jun Ueda is with d'Arbeloff Laboratory for Information Systems and Technology, Department of Mechanical Engineering, Massachusetts Institute of Technology, Cambridge, MA 02139. Tel: 617-253-3772, Fax: 617-258-6575, and also with the Graduate School of Information Science, Nara Institute of Science and Technology, Nara, 630-0192, Japan. E-mail: uedajun@is.naist.jp.

Ming Ding, Masayuki Matsugashita, Reishi Oya, and Tsukasa Ogasawara are with the Graduate School of Information Science, Nara Institute of Science and Technology, Nara, 630-0192, Japan.

Fig. 3 shows the comparison for 10 muscles, including the short head of biceps brachii (BICs), long head of triceps brachii (TRIs), brachioradialis (BRD), pronator teres (PRO), supinator (SUP), flexor carpi ulnaris (FCU), flexor carpi radialis (FCR), extensor carpi ulnaris (ECU), extensor carpi radialis longus (ECRl), and flexor digitorum superficialis (FDS). As can be seen in the figure, the values obtained by our model are sufficiently close to Lemay's approximate expressions. Note that Lemay *et al.* have given approximate expressions only for a limited number of muscles and basic postures with a single joint movement. The anatomical data of detailed muscle moment arms for the upper limb is difficult to obtain at the present moment; therefore the whole posture of the model has not been evaluated.

Strictly speaking, from a biomechanical point of view, the joint mechanism of the human is complicated and this mechanism can not be easily represented by a simple pin joint; likewise, the backbone and shoulder have complex structures. Moreover, the anatomical attachment points of muscles are distributed. In this paper, we apply a simplified model to avoid complexity and reduce computational time. Further improvement and evaluation of the model are necessary.

B. Power-assisting device and integrated model

A power-assisting device (exoskeleton) using pneumatic actuators shown in Fig. 4 (a) has been developed for modifying or *controlling* muscle force in the forearm. Eight pneumatic actuators with a 20 [mm] diameter, a maximum pressure of 0.4 [MPa], and a maximum force of 60 [N] are used. Both ends of each actuator are attached to plastic frames which are attached to the forearm by Velcro tapes. Electromagnetic valves shown in Fig. 4 (b) are used to control the pressure. Although pneumatic actuators have nonlinearities, the compactness and lightweightness excluding compressors are considered suitable for developing a device with multiple DOFs.

This device assists a 3 degrees of freedom (DOF) motion of the wrist and 1 DOF motion of the elbow by using 8 actuators. The models for these pneumatic actuators are added to the musculoskeletal human model as massless wires, composing the musculoskeletal-exoskeletal integrated human model shown in Fig. 5. The function of this device is to generate torques for 4 joints of the forearm described above. Note that the pneumatic actuators never directly assist the muscles beneath them; the driving-forces of the actuators are transmitted through the joints, and modify the wearer's muscle forces according to Crowninshield. Unlike human muscles, this device is not redundant hence the solution of the driving-forces is uniquely obtained for desired joint torques. The integrated human model calculates the length of each actuator during the motion. Then, stiffness and equilibrium point of the actuator are calculated for a given driving-force and the length, which finally gives a desired pressure.

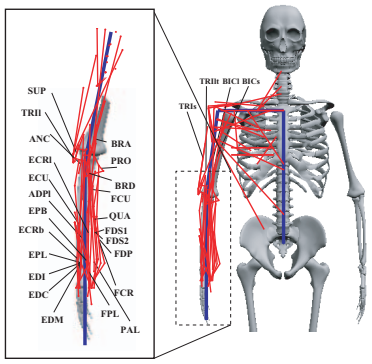

Fig. 2. Musculoskeletal model of upper right limb

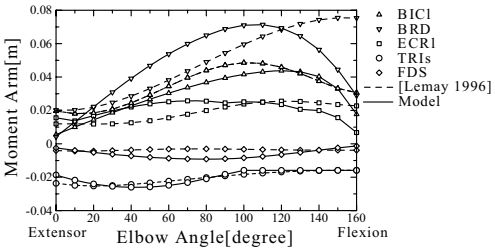

(a) Flexion/extensor of elbow

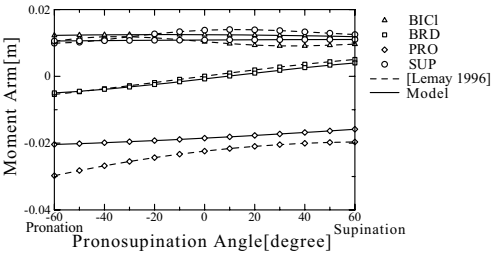

(b) Supination/pronation of elblow

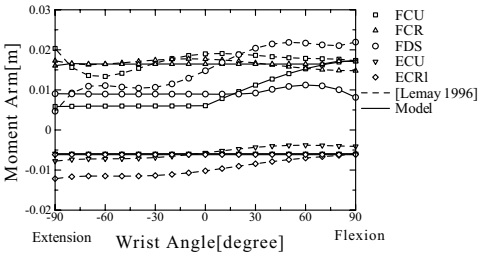

(c) Flexion/extension of wrist

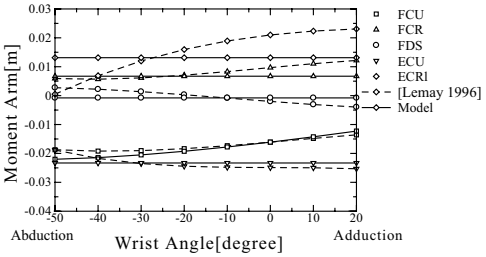

(d) Adduction/abduction of wrist

Fig. 3. Comparison of moment arms between the developed model and Lemay's model[6]

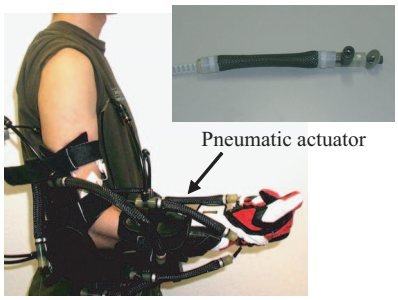

(a) Power-assisting device

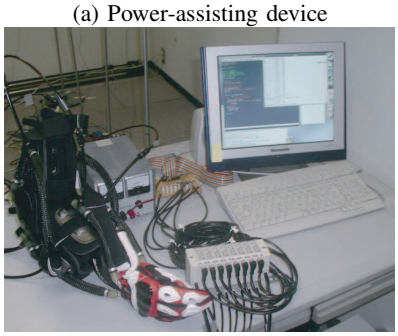

(b) Control system

Fig. 4. Experimental apparatus

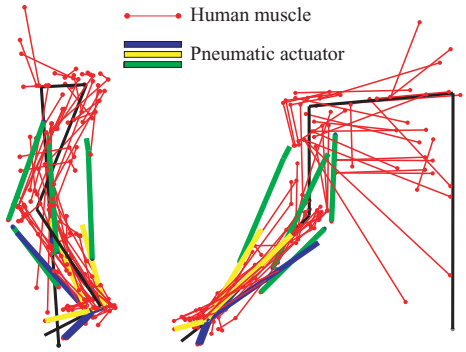

(a) Side view (b) Front view

Fig. 5. Musculoskeletal-exoskeletal integrated human model

III. Control of Muscle Force During Exercise

A. Cost function

Hereafter, we assume that the musculoskeletal-exoskeletal integrated human model has m skeletal muscles, n actuators, and l joints. Joint torque $\boldsymbol{\tau} = [\tau_1, \cdots, \tau_l]^T$ is given by:

$$\boldsymbol{\tau} = \boldsymbol{A}\boldsymbol{f} + \boldsymbol{E}\boldsymbol{p} \tag{1}$$

where $\boldsymbol{f} = [f_1, \cdots, f_m]^T$ and $\boldsymbol{p} = [p_1, \cdots, p_n]^T$ are contraction forces of muscles and driving-forces of actuators respectively. $\boldsymbol{A}$ is a moment arm matrix of muscles whose element a_{ij} denotes the moment arm of muscle j for joint i. $a_{ij} = 0$ is given if f_j does not affect joint i. $\boldsymbol{E}$ is a moment arm matrix of actuators.

The human body has a redundant number of muscles compared with that of joints, which makes the estimation of muscle forces from the joint torques an ill-posed problem. In order to cope with this problem, the following cost function is used as an extension of Crowninshield's cost function [3]:

$$u(\boldsymbol{f}, \boldsymbol{p}) \triangleq \sum_{j=1}^{m} \left(\frac{f_j}{PCSA_j} \right)^r + \sum_{j=1}^{n} \left(\frac{p_j}{C_j} \right)^r \tag{2}$$

where $PCSA_j$ is the physiological cross sectional area for muscle j, and C_j is the cross sectional area for actuator j. Crowninshield *et al.* has investigated various types of cost functions [3]. In this paper, a quadratic cost function is chosen, i.e., $r = 2$. The first term of (2) corresponds to the cost for the skeletal muscles, and the second term corresponds to the cost for the actuators. As will be shown in the following section, the load for the muscles and actuators are determined such that this cost function is minimized.

B. Muscle force control algorithm

The aim of the proposed algorithm is to arbitrarily modify the load force of selected muscles. Figure 6 shows the algorithm consisting of the following four steps. The first three steps calculate and check the muscle forces by using the integrated human model, and the fourth step performs the muscle force control by using the hardware. Note that our method proposed in this section is not dependent on the type of actuator as far as linear actuators are used.

[Step 1] Muscle force estimation during exercise First, a target motion is measured by a motion capture system. Joint torque $\boldsymbol{\tau}_0$ is calculated by substituting the obtained joint angles, velocities, and accelerations to the musculoskeletal model. The muscle force $\boldsymbol{f}_0$ for a target motion without using the exoskeleton are estimated by letting $\boldsymbol{p} = \boldsymbol{0}$ and minimizing the cost function:

$$u(\boldsymbol{f})|_{\boldsymbol{p}=\boldsymbol{0}} \rightarrow \min \tag{3}$$

subject to $\boldsymbol{\tau} = \boldsymbol{\tau}_0$, $0 \leq f_j \leq f_{j_{max}}$ $(j = 1, \cdots, m)$, and $p_j = 0$ $(j = 1, \cdots, n)$, where $f_{j_{max}} = \varepsilon \cdot PCSA_j$ $(j = 1, \cdots, m)$ is the maximum muscle force. $\varepsilon = 0.7 \times 10^6$[N/m^2] has been given by Karlsson[7]. $PCSA_j$'s are given from [8], [9]. The obtained muscle forces $\boldsymbol{f}_0$, hereafter called nominal force, is used as the basis for the designation of muscle forces in the next step.

[Step 2] Actuator driving-force calculation Based on the nominal muscle forces, a set of desired muscle forces f_{dj} is given by:

$$f_{dj} = \alpha_j f_{0j} \quad (j = 1, \cdots, m) \tag{4}$$

where $\alpha_j \geq 0$ is a design coefficient determined by the purpose of power-assisting, e.g., for training specific muscles, desired forces for the muscles are set larger than the nominal forces as $\alpha_j > 1$. Similarly, $0 \leq \alpha_j < 1$ denotes that the muscle force is supported, and $\alpha_j = 1$ denotes that the muscle force is not changed.

The driving-forces of the pneumatic actuators $\boldsymbol{p}_d$ that realize $\boldsymbol{f}_d$ are obtained by giving $\boldsymbol{f}_d$ as equality constraints for (2):

$$u(\boldsymbol{p})|_{\boldsymbol{f}=\boldsymbol{f}_d} \rightarrow \min \tag{5}$$

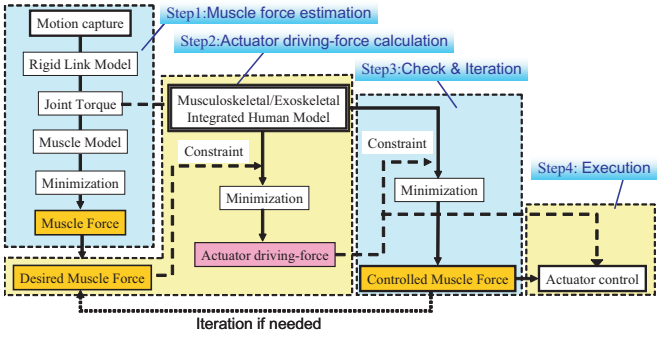

Fig. 6. Muscle force control algorithm

subject to $\boldsymbol{\tau} = \boldsymbol{\tau}_0$, $\boldsymbol{f} = \boldsymbol{f}_d$ and $0 \leq p_j \leq p_{j_{max}}$ $(j = 1, \cdots, n)$, where $C_j = 1.0 \times 10^{-4}\pi[\mathrm{m}^2]$ and $p_{j_{max}} = 60[\mathrm{N}]$ for $j = 1, \cdots, n$ are determined according to the specification of the pneumatic actuator.

[Step 3] Check and Iteration Muscle force estimation is once again conducted by setting the obtained driving forces of the pneumatic actuators, $\boldsymbol{p}_d$, as constraints for the minimization:

$$u(\boldsymbol{f})|_{\boldsymbol{p}=\boldsymbol{p}_d} \rightarrow \min \tag{6}$$

subject to $\boldsymbol{\tau} = \boldsymbol{\tau}_0$, $0 \leq f_j \leq f_{j_{max}}$ $(j = 1, \cdots, m)$, and $\boldsymbol{p} = \boldsymbol{p}_d$. If the result $\hat{\boldsymbol{f}}$ is unsatisfactory, a return to the step 2 modifies the desired muscle forces.

[Step 4] Execution of motion support/training by activating the Exoskeleton The power-assisting device is activated according to desired pressure calculated from the actuator-driving forces.

Remark 1 Motion capturing in Step 1 is unnecessary if the target motion can be obtained by different methods, e.g., motion generation software.

Remark 2 Time-varying design coefficients, $\alpha_j(t)$, can be applied in Step 2.

Remark 3 Since many muscles are highly coupled with each other, an arbitrary set of muscle forces can not be realized; a feasible set of muscle forces needs to be designated in Step 2.

Remark 4 At this point, this algorithm is difficult to perform *online* since it requires minimizations for three times. Therefore, only pre-calculated motion patterns can be executed.

IV. Feasibility of Muscle Force Control

This section analyzes the feasibility of the muscle force control by using power-assisting device.

A. Condition of optimality

Consider the optimization problem described by (3). For simplicity, the inequality conditions $f_j \leq f_{j_{max}}$ $(j = 1, \cdots, m)$ are omitted. The Kuhn-Tucker theorem [10] implies that a solution $\boldsymbol{f}$ for the optimization problem must satisfy

$$\nabla u(\boldsymbol{f}) + \sum_{i=1}^{l} \mu_i \nabla h_i(\boldsymbol{f}) + \sum_{j=1}^{m} \lambda_j \nabla g_j(\boldsymbol{f}) = 0 \tag{7}$$

$$h_i(\boldsymbol{f}) = 0 \quad (i = 1, 2, \cdots, l) \tag{8}$$

$$\lambda_j g_i(\boldsymbol{f}) = 0, \lambda_j \geq 0, g_j(\boldsymbol{f}) \leq 0 \ (j = 1, 2, \cdots, m) \tag{9}$$

where $h_i(\boldsymbol{f}) = \tau_i - \boldsymbol{a}_i^T \boldsymbol{f}$ and $g_j(\boldsymbol{f}) = -f_j$. $\boldsymbol{a}_i \in \Re^m$ is a column vector of $\boldsymbol{A}$, i.e., $\boldsymbol{A} = [\boldsymbol{a}_1 \boldsymbol{a}_2 \cdots \boldsymbol{a}_l]^T$, and

$$\frac{\partial u(\boldsymbol{f})}{\partial f_j} = r \left(\frac{f_j}{PCSA_j} \right)^{r-1} \triangleq q_j \tag{10}$$

$$\frac{\partial h_i(\boldsymbol{f})}{\partial f_j} = a_{ij} \tag{11}$$

$$\frac{\partial g_j}{\partial f_k} = \begin{cases} -1, & j = k \\ 0, & j \neq k \end{cases} \tag{12}$$

Therefore, (7) can be written as

$$\boldsymbol{q} = \boldsymbol{A}^T \boldsymbol{\mu} + \boldsymbol{\lambda} \tag{13}$$

where $\boldsymbol{q} = [q_1, q_2, \cdots, q_m]^T$, $\boldsymbol{\mu} = [\mu_1, \mu_2, \cdots, \mu_l]^T$, and $\boldsymbol{\lambda} = [\lambda_1, \lambda_2, \cdots, \lambda_m]^T$.

Recall $\lambda_j = 0$ if $f_i > 0$. Let k be the number of nonzero elements of $\boldsymbol{f}$. The following equation is obtained by a permutation of the rows of (13):

$$\begin{bmatrix} \tilde{\boldsymbol{q}} \\ \hline \boldsymbol{0} \end{bmatrix} = \begin{bmatrix} \tilde{\boldsymbol{A}}_u \\ \hline \boldsymbol{A}_v \end{bmatrix} \boldsymbol{\mu} + \begin{bmatrix} \boldsymbol{0} \\ \hline \tilde{\boldsymbol{\lambda}} \end{bmatrix} \tag{14}$$

where all elements of $\tilde{\boldsymbol{q}} \in \Re^k$ and $\tilde{\boldsymbol{\lambda}} \in \Re^{(m-k)}$ are nonnegative, $\tilde{\boldsymbol{A}}_u \in \Re^{k \times l}$ and $\tilde{\boldsymbol{A}}_v \in \Re^{(m-k) \times l}$. Step 1 of the muscle control algorithm (muscle force estimation) gives $\boldsymbol{f}_0$ as a solution of (3). Since the function $u(\boldsymbol{f})|_{\boldsymbol{p}=\boldsymbol{0}}$ is convex, $\boldsymbol{f}_0$ is unique. This $\boldsymbol{f}_0$ satisfies

$$\boldsymbol{\tau}_0 = \boldsymbol{A}\boldsymbol{f}_0, \tag{15}$$

$$\boldsymbol{q}_0 = \boldsymbol{A}^T \boldsymbol{\mu}_0 + \boldsymbol{\lambda}_0 \tag{16}$$

where $\boldsymbol{q}_0$ is uniquely obtained from $\boldsymbol{f}_0$, i.e.,

$$q_{0j} = r \left(\frac{f_{0j}}{PCSA_j} \right)^{r-1} \quad (j = 1, \cdots, m). \tag{17}$$

$\boldsymbol{\mu}_0$ and $\boldsymbol{\lambda}_0$ that satisfy (16) is obtained accordingly. Similarly, (16) can be permutated as

$$\begin{bmatrix} \tilde{\boldsymbol{q}}_0 \\ \hline \boldsymbol{0} \end{bmatrix} = \begin{bmatrix} \tilde{\boldsymbol{A}}_u \\ \hline \boldsymbol{A}_v \end{bmatrix} \boldsymbol{\mu}_0 + \begin{bmatrix} \boldsymbol{0} \\ \hline \tilde{\boldsymbol{\lambda}}_0 \end{bmatrix}. \tag{18}$$

B. Feasibility of muscle force control

The muscle force control is a method to realize $\boldsymbol{f}_d$ by applying the joint torques $\boldsymbol{\tau}_a = \boldsymbol{E}\boldsymbol{p}_d$ from the power-assisting device. The aim of the following analysis is to clarify the class of feasible $\boldsymbol{f}_d$. We assume that (a) the power-assisting device can generate arbitrary torques at all joints, i.e., all components of $\boldsymbol{\tau}$ can be modified arbitrarily, and (b) we control the muscles whose nominal forces are also positive, i.e., we keep the muscles unchanged whose nominal forces are zero. The latter assumption holds if the desired muscle forces are determined according to (4).

Theorem: Muscle force control

Let $\boldsymbol{w}(\boldsymbol{q}) = \boldsymbol{f}$ be a function that maps $\boldsymbol{q}$ to the corresponding $\boldsymbol{f}$. (Roughly speaking, $\boldsymbol{w}$ is an inverse function of (17).) Note that $\boldsymbol{w}(\boldsymbol{q}) = \boldsymbol{w}(\tilde{\boldsymbol{q}})$, e.g., $\boldsymbol{f}_0 = \boldsymbol{w}(\tilde{\boldsymbol{q}}_0)$. Suppose $\boldsymbol{\lambda}_0$ exists. Also suppose $\exists \boldsymbol{\alpha} \in \Re^m$ such that all the elements of $\tilde{\boldsymbol{\lambda}}_0 - \tilde{\boldsymbol{A}}_v \boldsymbol{\alpha}$ remain nonnegative. Then, the feasible set of $\boldsymbol{f}_d$ is represented by

$$\boldsymbol{f}_d = \boldsymbol{w}\left(\tilde{\boldsymbol{q}}_0 + \tilde{\boldsymbol{A}}_u \boldsymbol{\alpha}\right) \tag{19}$$

where $\boldsymbol{\alpha}$ is a free parameter for determining the desired muscle forces. The desired muscle forces $\boldsymbol{f}_d$ is realized if the power-assisting device exerts the following torque

$$\boldsymbol{\tau}_a = \boldsymbol{A}\boldsymbol{f}_d - \boldsymbol{\tau}_0. \tag{20}$$

Note that $\boldsymbol{\alpha}$ can be chosen freely if $\boldsymbol{\lambda}_0$ does not exist.

Proof: It is enough to show the existence of $\boldsymbol{\mu}_d$ and $\tilde{\boldsymbol{\lambda}}_d$ that satisfy (13) for the proof. Let $\boldsymbol{\mu}_d = \boldsymbol{\mu}_0 + \boldsymbol{\alpha}$ and $\tilde{\boldsymbol{\lambda}}_d = \tilde{\boldsymbol{\lambda}}_0 - \tilde{\boldsymbol{A}}_v \boldsymbol{\alpha}$. These parameters satisfy (13) since

$$\begin{aligned}
\begin{bmatrix} \tilde{\boldsymbol{q}}_d \\ \hline \boldsymbol{0} \end{bmatrix} &= \begin{bmatrix} \tilde{\boldsymbol{q}}_0 + \tilde{\boldsymbol{A}}_u \boldsymbol{\alpha} \\ \hline \boldsymbol{0} \end{bmatrix} \\
&= \begin{bmatrix} \tilde{\boldsymbol{A}}_u \\ \hline \tilde{\boldsymbol{A}}_v \end{bmatrix} \boldsymbol{\mu}_0 + \begin{bmatrix} \boldsymbol{0} \\ \hline \tilde{\boldsymbol{\lambda}}_0 \end{bmatrix} + \begin{bmatrix} \tilde{\boldsymbol{A}}_u \\ \hline \tilde{\boldsymbol{A}}_v \end{bmatrix} \boldsymbol{\alpha} + \begin{bmatrix} \boldsymbol{0} \\ \hline -\tilde{\boldsymbol{A}}_v \boldsymbol{\alpha} \end{bmatrix} \\
&= \begin{bmatrix} \tilde{\boldsymbol{A}}_u \\ \hline \tilde{\boldsymbol{A}}_v \end{bmatrix} \boldsymbol{\mu}_d + \begin{bmatrix} \boldsymbol{0} \\ \hline \tilde{\boldsymbol{\lambda}}_d \end{bmatrix} \square.
\end{aligned} \tag{21}$$

The number of joints is merely l, which is generally less than the number of muscles. This implies that theoretically it is impossible to arbitrarily choose and control a single muscle out of k muscles since the degrees of freedom of the muscle control is limited by $\mathrm{rank}(\tilde{\boldsymbol{A}}_u) \leq l$. In other words, some muscle forces may change due to the lack of the degrees of freedom. However, practically, some application may allow this change of small muscles which do not much contribute to the motion. A set of initial desired forces can be determined by this analysis, and a set of practical controlled muscle forces is examined by the muscle control algorithm.

V. Example

A. Control of muscle force by the integrated model (Steps 1 to 3)

The elbow flexion/extension shown in Fig. 7 is considered as an example. Figure 8 (a) shows the muscle forces estimated from the motion without the exoskeleton. In this example, loads for the brachialis and brachioradials are modified; desired muscle forces are given as shown in Fig. 8 (b), in which only the loads for the brachialis and brachioradials are set to half of the nominal values, and the other muscles are set to unchanged. In step 2 of the proposed algorithm, the driving forces of the actuators, which realize the desired muscle forces, are obtained. Figure 8 (c) shows the muscle forces when the exoskeleton is activated. The loads of the brachialis and brachioradials become approximately 60% of the nominal forces, and the other muscles remain almost unchanged.

Fig. 7. Elbow flexion and extension

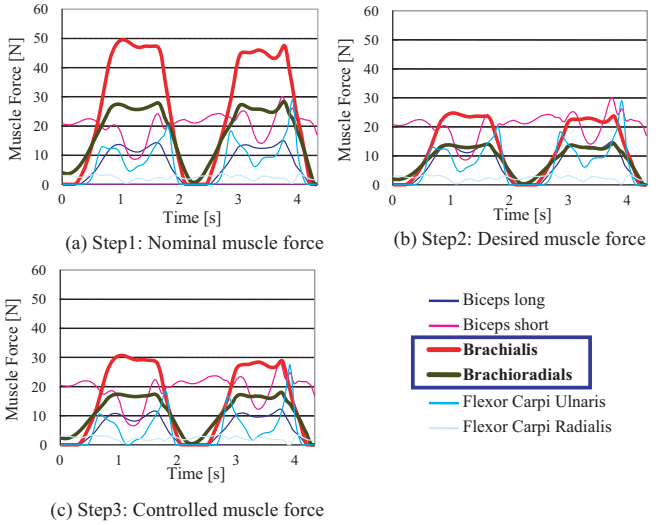

(a) Step1: Nominal muscle force

(b) Step2: Desired muscle force

(c) Step3: Controlled muscle force

Fig. 8. Muscle forces for the elbow flexion/extension obtained from the integrated model: Brachialis and Brachioradials x 0.5, others x 1 (no change)

The desired muscle forces have not been realized completely; however, the ratio between the nominal and controlled muscles is satisfactorily close to the designated value, which is 50%. Some muscle forces change even though these muscles are set unchanged; e.g., the biceps long and flexor carpi ulnaris are affected by the muscle force control and changed approximately 75%, which means that these muscles couple with the controlled muscles to some extent. In contrast, the biceps short and the flexor carpi radialis are unchanged. The loads of the brachialis and brachioradials can be changed without largely changing the loads of other muscles. As will be understood, the degree of muscle coupling is not easy to analyze since it is dependent upon posture and motion.

B. Experiment (Step 4)

Two types of experiments were conducted, by activating the power-assisting device:

- Experiment 1 (motion support): Brachialis and brachioradials were set to *zero*, and the other muscles were set to unchanged.
- Experiment 2 (training): Brachialis and brachioradials were set to twice of the nominal forces, and the other muscles were set unchanged.

These desired values were given in step 2 of the proposed algorithm, and the driving forces of the actuators were calculated. One male subject performed the elbow motion 10 times starting from flexion followed by extension in 2 seconds. The surface EMGs during motion were measured

TABLE I

MEAN (STANDARD ERROR) OF EMG FOR EXPERIMENT 1: BRACHIALIS AND BRACHIORADIALS X 0.0, OTHERS X 1.0

Muscle name	Brachialis	Brachioradials	Biceps short	Flexor Carpi Ulnaris
Desired ratio in step 2	0.0	0.0	1.0	1.0
Obtained ratio in step 3	0.187	0.248	0.889	0.443
Normalized EMG	0.739 (0.081)	0.784 (0.058)	1.1405 (0.051)	0.839 (0.034)

TABLE II

MEAN (STANDARD ERROR) OF EMG FOR EXPERIMENT 2: BRACHIALIS AND BRACHIORADIALS X 2.0, OTHERS X 1.0

Muscle name	Brachialis	Brachioradials	Biceps short	Flexor Carpi Ulnaris
Desired ratio in step 2	2.0	2.0	1.0	1.0
Obtained ratio in step 3	1.721	1.696	1.208	1.605
Normalized EMG	1.550 (0.767)	1.641 (0.581)	1.664 (0.442)	2.479 (1.534)

for brachialis, brachioradials, biceps short, and flexor carpi ulnaris for validation. The linear envelope of the EMGs were calculated by taking the absolute value and applying a low-pass filter. Figure 9 shows typical examples of the EMG signals. As can be observed in the figure, the EMG signals of the controlled muscles, i.e., (a) brachialis and (b) brachioradials, in the experiment 1 (motion support) became smaller than that of the nominal ones. Similarly, the EMG signals in experiment 2 (training) became larger than that of the nominal ones. The signals of (c) biceps short and (d) flexor carpi ulnaris for experiment 1 did not show significant differences from the nominal ones as expected and the signals for experiment 2 fell short of the expectation.

Table I and II show the ratios between the time average of the nominal and obtained muscle forces. The obtained ratios for brachialis and brachioradials were considered sufficiently close to the desired ratios. The normalized EMG signals for brachialis and brachioradials show expected changes corresponding to the desired ratios, although the results were not satisfactorily compared with the results of step 3. The obtained value for biceps short did not largely change and flexor carpi ulnaris changed to the extent as previously described. The same tendency can be observed for the normalized EMG signals. At this time, the EMG signals for experiment 2 shown in Table II vary widely. The developed hardware is a prototype and has many points to be improved, e.g., the forces generated by the actuators cannot be transmitted to the human arm completely, due to imperfect attachment of the device and inaccurate control of pressure.

VI. CONCLUSION

A concept of muscle force control has been presented. A muscle force control algorithm has been proposed to modify the load of selected muscles by using an exoskeleton, thus enabling "pinpointed" motion support, rehabilitation, and training. An advanced dynamic model, called the musculoskeletal-exoskeletal integrated human model, has been developed. Experiments have been conducted by using a power-assisting device with pneumatic actuators. The validity of the method has been confirmed by measuring surface EMG signals. Future work includes the analysis of muscle coupling, and improvement of the hardware.

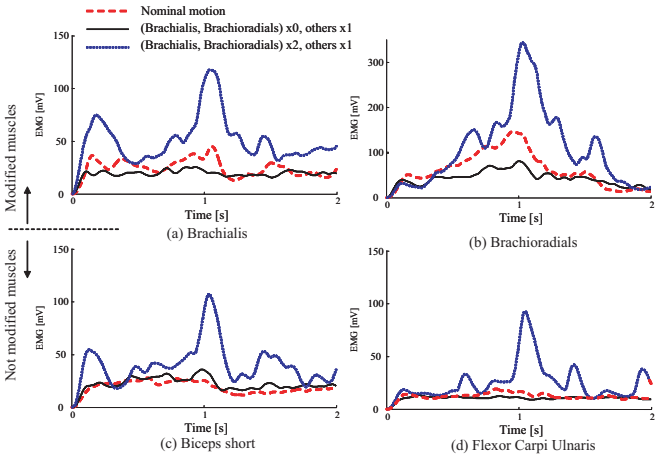

Fig. 9. Experimental results: comparison of EMG signals

REFERENCES

[1] H. Kazerooni, "Extender: A Case Study for Human-Robot Interaction via Transfer of Power and Information Signals," Proc. IEEE Int. Workshop on Robot and Human Communication, pp. 10-20, 1993.

[2] S. Lee and Y. Sankai, "Power Assist Control for Walking Aid with HAL-3 Based on EMG and Impedance Adjustment around Knee Joint," Proc. IEEE/RSJ Int. Conf. Intelligent Robots and Systems, 1499-1504, 2002.

[3] R. D. Crowninshield and R. A. Brand, "A physiologically based criterion of muscle force prediction in locomotion", J. Biomechanics, 14, 793-801, 1981.

[4] W. Maurel and D. Thalmann, "A Case Study on Human Upper Limb Modelling for Dynamic Simulation," Computer Methods in Biomechanics and Biomechanical Engineering, 2(1), 65-82, 1999.

[5] S. L. Delp, et al, "An interactive graphics-based model of the lower extremity to study orthopaedic surgical procedures," IEEE Trans. Biomedical Engineering, Vol. 37, Issue 8, 757-767, 1990.

[6] M. A. Lemay, P. E. Crago, "A dynamic model for simulating movements of the elbow, forearm, and wrist," J. Biomechanics, 29, 1319-1330, 1996.

[7] D. Karlsson and B. Peterson, "Towards a model for force predictions in the human shoulder", J. Biomechanics, 25, 189-199, 1992.

[8] MotCo project, http://www.motco.dir.bg/Data/PCSA.html.

[9] H. E. J. Veeger et al. , "Inertia and muscle contraction parameters for musculoskeletal modelling of the shoulder mechanism," J. Biomechanics, 24, 615-629, 1991.

[10] *Nonlinear Programming*, D. Bertsekas, 2nd edition, Athena Scientific, 1999.